Expression of Bcl-x_L and loss of p53 can cooperate to overcome a cell cycle checkpoint induced by mitotic spindle damage

Andy J. Minn,[1,2] Lawrence H. Boise,[1] and Craig B. Thompson[1–4]

[1]Gwen Knapp Center for Lupus and Immunology Research, [2]The Committee on Immunology, [3]Howard Hughes Medical Institute, Department of Medicine, and Department of Molecular Genetics and Cell Biology, The University of Chicago, Chicago, Illinois 60637 USA

During somatic cell division, faithful chromosomal segregation must follow DNA replication to prevent aneuploidy or polyploidy. Damage to the mitotic spindle is one potential mechanism that interferes with chromosomal segregation. The accumulation of aneuploid or polyploid cells resulting from a disrupted mitotic spindle is presumably prevented by cell cycle checkpoint controls. In the course of studying cells that overexpress the apoptosis-inhibiting protein Bcl-x_L, we found that these cells have an increased rate of spontaneous tetraploidization, suggesting that apoptosis may play an important role in eliminating cells that fail to complete mitosis properly. When cells expressing Bcl-x_L are treated with mitotic spindle inhibitors, a significant percentage reinitiate DNA replication and become polyploid. Nevertheless, the majority of cells expressing Bcl-x_L undergo a prolonged p53-dependent cell cycle arrest following mitotic spindle damage. Unexpectedly, p53 expression is not induced in mitosis, nor does it influence M-phase arrest. Instead, cells with mitotic spindle damage only transiently arrest in M phase, and despite failing to complete mitosis, appear to proceed to G_1. During this subsequent growth factor-dependent phase, p53 is induced and mediates cell cycle arrest. In cells that do not overexpress Bcl-x_L, elimination of the p53-dependent growth arrest with a dominant negative mutant also results in polyploidy after mitotic spindle damage, but under these conditions most cells die by apoptosis. Expression of Bcl-x_L and abrogation of p53 cooperate to allow rapid and progressive polyploidization following mitotic spindle damage. Our results suggest that suppression of apoptosis by *bcl-2*-related genes and loss of p53 function can act cooperatively to contribute to genetic instability.

[*Key Words*: Apoptosis; checkpoint control; mitosis; mitotic spindle; p53; Bcl-x_L]

Received April 4, 1996; revised version accepted August 28, 1996.

During cell division, the orderly execution of DNA replication and chromosomal segregation, which define the S and M phases of the cell cycle, respectively, must occur with great fidelity. To ensure the interdependency of S phase and M phase, cells have developed mechanisms to monitor the completion of each process and halt cell cycle progression if either process is interrupted by cellular damage. Presumably, arresting damaged cells gives them a chance to repair and/or prevents their further expansion. Cell cycle checkpoint controls are genetic pathways that include proteins that sense damage, arrest the cell cycle, initiate repair, and cause apoptosis (Murray 1994, 1995). The importance of genes involved in these pathways is emphasized by the increasing evidence that mutations in checkpoint control genes contribute to tumorigenesis and by the fact that cancer cells often have karyotypic abnormalities (Hartwell and Kastan 1994).

p53 is one of the best-studied proteins involved in cell cycle checkpoint controls and is found to be mutated in over half of all human cancers (Hollstein et al. 1991). After DNA damage, p53 is induced and acts as a sequence-specific transcription factor (Cox and Lane 1995; Haffner and Oren 1995). The cyclin dependent kinase inhibitor $p21^{Waf1/Cip1}$ is a direct transcriptional target of p53 transactivation and is partly responsible for arresting cells in G_1 (El-Deiry et al. 1993; Harper et al. 1993; Deng et al. 1995). Gadd45 is another transcriptional target and is involved in stimulating DNA repair (Smith et al. 1994). Besides its role in a G_1 checkpoint, p53 also has

[4]Corresponding author.

been implicated in having a role in G_2/M. Fibroblasts null for p53 rapidly become aneuploid and polyploid in culture (Harvey et al. 1993), and after mitotic spindle damage these cells continue DNA replication in the absence of cell division and become polyploid (Cross et al. 1995). Interestingly, arrest after mitotic spindle damage is not dependent on $p21^{Waf1/Cip1}$ (Deng et al. 1995).

Apoptosis is also being recognized as an important genetic mechanism in controlling cancer. Increasing the apoptotic threshold may be important for tumor growth because, in addition to causing proliferation, oncogene expression is often associated with increased programmed cell death (Evan et al. 1995). Additionally, an elevated apoptotic threshold contributes to radiation and chemotherapy resistance (Fisher 1994). p53 is also able to mediate apoptosis. Loss of p53 prevents thymocytes from undergoing apoptosis after gamma irradiation (Clarke et al. 1993; Lowe et al. 1993b) and decreases the efficacy of chemotherapy in vitro (Lowe et al. 1993a) and in vivo (Lowe et al. 1994). Loss of p53-mediated apoptosis also potentially contributes to tumorigenesis in conjunction with the loss of tumor suppressor genes such as *rb* (Haffner and Oren 1995) or the gain of oncogenes such as c-*myc* (Evan et al. 1995).

The inappropriate expression of antiapoptosis genes including members of the *bcl-2* family is another way to raise the apoptotic threshold of cancer cells (Hockenbery 1995). Overexpression of either Bcl-2 or the related protein Bcl-x_L can protect tumor cells from a wide variety of apoptotic stimuli and confers a multidrug resistance phenotype (Miyashita and Reed 1993; Dole et al. 1994; Minn et al. 1995). Recent evidence shows that Bcl-x_L can be highly expressed in both primary tumors and tumor cell lines (Dole et al. 1995; Schlaifer et al. 1995).

One function of cell cycle checkpoints is to prevent the expansion of cells with unrepaired genetic damage. In theory, mutations in any of numerous genes involved in a checkpoint pathway could result in accumulation of damaged cells. These include genes involved in sensing the damage, causing cell cycle arrest, initiating repair, or inducing apoptosis. Whether most cell cycle checkpoint controls are simple linear pathways or involve several independent pathways remains unclear. In a linear pathway, apoptosis may require cell cycle arrest, and simply disrupting the arrest mechanism may prevent death and allow expansion of damaged cells. Alternatively, if arrest and apoptosis are controlled independently, disrupting cell cycle arrest would still allow damaged cells to undergo apoptosis. Independent control of cell cycle arrest and apoptosis predicts that the expansion of cells with abnormalities would occur only if both pathways are perturbed, a prediction that is in accord with a multihit model of carcinogenesis. In the work presented here, we address these issues in the context of a cell cycle checkpoint that is responsive to mitotic spindle damage. Damage induced by agents that disrupt the mitotic spindle initiates a p53-dependent cell cycle arrest and causes apoptosis in a manner that is p53-independent and inhibitable by Bcl-x_L.

Results

Cells expressing Bcl-x_L have an increased propensity to become polyploid

Cells transfected with *bcl-x_L*, an antiapoptosis gene, have an increased propensity to become tetraploid after passage in cell culture when compared with cells transfected with a control vector. This was first noticed when the DNA content of murine FL5.12 cells transfected with *bcl-x_L* was measured during continuous passage in vitro. Using starting diploid clones, these cells often became tetraploid after only 2–3 weeks of culture.

These initial observations prompted us to further explore the relationship between Bcl-x_L expression and mechanisms involved in the control of ploidy. To assess whether Bcl-x_L enhanced the rate of spontaneous tetraploidization, FL5.12 cells were transfected with either a Bcl-x_L expression vector (FL5-Bcl-x_L) or a Neo control vector (FL5-Neo). These bulk transfected populations were then cloned by limiting dilution, and after expansion, the percentage of tetraploid clones was examined. After limiting dilution cloning, 30.2% of the expanded FL5-Bcl-x_L clones were tetraploid, compared with 4.2% of the expanded FL5-Neo clones (Table 1). This result suggests that Bcl-x_L expression is able to enhance the rate of spontaneous tetraploidization.

One way cells can become tetraploid is through disruption of the mitotic spindle and the failure of checkpoint controls to either arrest or repair the cells. To determine whether Bcl-x_L influenced the fidelity of a mitotic spindle checkpoint, we treated FL5-Neo and FL5-Bcl-x_L cells with nocodazole, a drug which disrupts the mitotic spindle by inhibiting microtubule polymerization. As seen in Figure 1, both FL5-Neo and FL5-Bcl-x_L cells arrested with a predominantly 4N DNA content after 24 hr of nocodazole exposure. This implies that Bcl-x_L does not affect the initial ability of checkpoint controls to arrest cells in M phase in response to mitotic spindle disruption. During the arrest, FL5-Neo cells rapidly lost viability in the presence of nocodazole. By 72 hr, <10% of FL5-Neo cells were viable, and of those viable cells 15% had escaped the cell cycle arrest to give rise to cells with a greater than 4N DNA content. In contrast, cells expressing Bcl-x_L were ~75% viable after 72 hr of nocodazole treatment and 40% of those cells had a

Table 1. *Spontaneous tetraploidization in cells expressing Bcl-x_L*

Cell type	Number of clones analyzed	Number tetraploid	Percent tetraploid
FL5-Neo	48	2	4.2
FL5-Bcl-x_L	76	23	30.2[a]

FL5.12 cells were transfected with either a Bcl-x_L expression vector (FL5 Bcl-x_L) or an empty Neo control vector (FL5-Neo). After selection, the bulk transfectants were cloned by limiting dilution. Clones were expanded and processed for DNA content analysis by flow cytometry.
[a] $P < 0.01$.

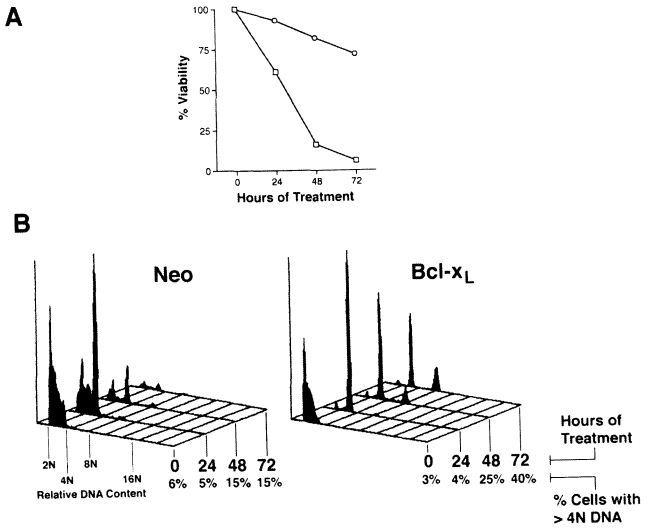

Figure 1. Bcl-x_L expression promotes the accumulation of polyploid cells after mitotic spindle damage. FL5.12 cells were stably transfected with the pSFFV-Neo expression vector with a Bcl-x_L cDNA insert (Bcl-x_L) (○) and an empty expression vector as a control (Neo) (□). Cells were treated with nocodazole for the indicated times. (*A*) At each time, cells were harvested and viability was quantitated by determining the percentage of sub-diploid cells. (*B*) Cells were also processed for cell cycle analysis by flow cytometry of propidium iodide-stained cells. Shown are three-dimensional representations of overlaid DNA histograms. The x-axis corresponds to relative DNA content, as marked on the left graph. The z-axis represents hr of nocodazole treatment, as marked, and below these markings is the percentage of cells with a >4N DNA content. These data are representative of at least three independent experiments.

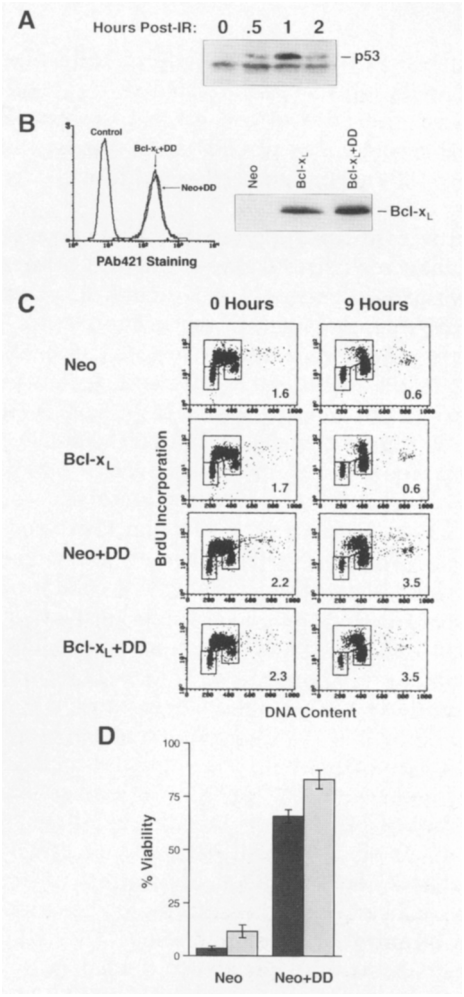

Figure 2. FL5.12 cells have functional p53 and a dominant negative p53 protein is able to abrogate both p53-dependent cell cycle arrest and p53-dependent apoptosis. (*A*) FL5-Neo cells were gamma irradiated at 5 Gy. At the indicated times postirradiation, cell lysates were made and analyzed by immunoblotting for p53. The position of p53 is indicated. The lower band seen on the blot is the result of nonspecific hybridization of the antibody. (*B*) FL5.12 cells were stably cotransfected with a Bcl-x_L expression vector and a DD expression vector (Bcl-x_L + DD) or an empty expression vector and a DD expression vector (Neo + DD). Clones were derived by limiting dilution. (*Left*) Expression levels of DD for two representative clones determined by flow cytometry of cells intracellularly stained using PAb421, an anti-p53 antibody that recognizes DD and endogenous p53. (*Right*) Immunoblot demonstrating expression levels for Bcl-x_L. (*C*) The indicated cells were gamma irradiated at 5 Gy and pulsed with BrdU at 0 and 9 hr postirradiation. Two-color cell cycle analysis using flow cytometry is presented with BrdU incorporation on the *y*-axis and propidium iodide DNA staining on the *x*-axis. Gates are drawn around the G_1, S, and G_2/M cell cycle populations. The *bottom left* gate is G_1; the *top* gate is S; and the *bottom right* gate is G_2/M. The number in the *lower right-hand* corner of each graph is the ratio of the percentage of cells in S to the percentage of cells in G_1. (*D*) The survival of FL5-Neo (Neo) and FL5-Neo + DD (Neo + DD) cells following treatment with either 1 μg/ml of etoposide (dark gray bars) or by irradiating with 5 Gy gamma radiation (light gray bars) was assayed as described in Materials and Methods. Shown is cell viability at 18 hr calculated as a percentage of an untreated control (means±standard deviations, $n=4$).

greater than 4N DNA content. These experiments yielded similar results when done with various doses of nocodazole or vincristine (data not shown). Additionally, when nocodazole or vincristine was removed from FL5-Bcl-x_L cells at 48 and 72 hr of treatment, cells reinitiated exponential growth and the majority of the recovered cells were tetraploid. In contrast, the recovered FL5-Neo cells remained mainly diploid (data not shown).

FL5.12 Cells have functional p53

Because it has been reported previously that cells mutated or null for p53 have elevated rates of polyploidy and aneuploidy, the p53 status of FL5.12 cells was investigated. The best characterized role for p53 is in the G_1 arrest following DNA damage (Kastan et al. 1992; Kuerbitz et al. 1992). Thus, FL5-Neo and FL5-Bcl-x_L cells were irradiated with 5 Gy gamma radiation and analyzed for p53 induction and p53-dependent G_1 arrest. FL5.12 cells rapidly and transiently induced p53 protein after irradiation (Figure 2A). p53 protein levels peaked between 30 min and 2 hr and returned to basal levels shortly thereafter. When an asynchronous population of either FL5-Neo or FL5-Bcl-x_L cells was irradiated, cell cycle analysis by bromodeoxyuridine (BrdU) incorporation and DNA staining demonstrated that at 9 hr postir-

radiation both FL5-Neo and FL5-Bcl-x_L cells showed a distinct population of cells arrested in G_1 (Figure 2C). Furthermore, the ratio of the percentage of cells in S phase to the percentage of cells in G_1 phase decreased from 1.6 to 0.6 in FL5-Neo cells and from 1.7 to 0.6 in FL5-Bcl-x_L cells.

To further confirm the presence of functional p53 in FL5.12 cells, we wished to show that the G_1 arrest phenotype was p53-dependent. For this purpose, a dominant negative p53 miniprotein (DD) that comprises the last 89 amino acids of wild-type murine p53 was used (Shaulian et al. 1992). DD oligomerizes with endogenous p53 and inhibits p53 from binding to its DNA consensus site. FL5.12 cells were cotransfected with either a DD expression vector and a Bcl-x_L expression vector or a DD expression vector and a Neo control vector to create the stable cell lines FL5-Bcl-x_L + DD and FL5-Neo + DD, respectively. Clones of each cell line were screened for expression of DD by flow cytometry of cells intracellularly stained with PAb421, an anti-p53 antibody that recognizes both DD and the endogenous p53 stabilized by DD. FL5-Bcl-x_L + DD and FL5-Neo + DD clones that stained similarly with PAb421 were chosen. Additionally, the FL5-Bcl-x_L + DD clones expressed similar levels of Bcl-x_L compared with the FL5-Bcl-x_L cells. Several clones were characterized, but shown here are representative clones of FL5-Neo + DD and FL5-Bcl-x_L + DD (Figure 2B). As seen in Figure 2C, DD effectively abrogated the DNA damage-induced G_1 arrest in both Neo and Bcl-x_L backgrounds, as indicated by the increase in the S to G_1 ratio 9 hr postirradiation.

Because p53 has also been shown to mediate apoptosis in response to DNA damage, the ability of FL5.12 cells to undergo p53-dependent apoptosis after either irradiation or treatment with etoposide was examined. As seen in Figure 2D, FL5-Neo cells rapidly died after either etoposide treatment or irradiation. Stable transfection of the DD minigene was able to inhibit cell death under these conditions. Thus, the p53 expressed by FL5.12 cells is capable of inducing G_1 cell cycle arrest and promoting apoptosis in response to DNA damage.

p53 is induced in cells after mitotic spindle damage

Knowing that FL5.12 cells express functional p53 and that p53 has been implicated in G_2/M checkpoint controls, we determined whether p53 was induced after treatment with nocodazole. FL5-Bcl-x_L cells were treated with nocodazole for 72 hr, and p53 expression was analyzed by immunoblotting (Figure 3A). p53 was induced and peaked between 8 and 48 hr of treatment. By 72 hr, p53 levels declined despite the continuous presence of nocodazole. p53 induction was similar in FL5-Neo cells (data not shown).

As a test for p53 function after nocodazole treatment, FL5-Bcl-x_L cells were transfected with a CAT reporter construct that contained p53-specific DNA binding sites upstream of the promoter. Figure 3B demonstrates that p53 transactivated the reporter, and that this transactivation was induced more than threefold by nocodazole

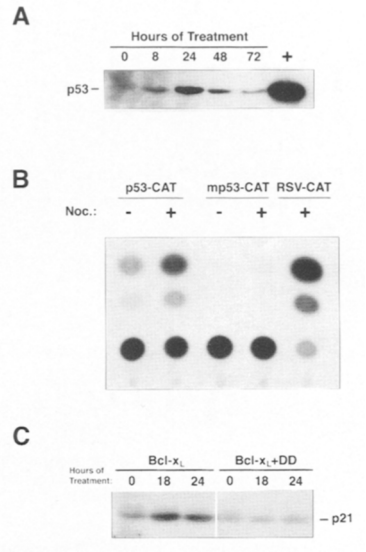

Figure 3. p53 is induced and able to transactivate gene expression after mitotic spindle damage. (*A*) FL5-Bcl-x_L cells were cultured with nocodazole for the indicated times. At each time, cell lysates were made and analyzed by immunoblotting for p53. (+) Positive control lane for p53. (*B*) FL5-Bcl-x_L cells were transfected with CAT reporter constructs and either left in media alone (−) or treated with nocodazole (Noc.) 6 hr after transfection (+). Cells were harvested for CAT assay at 48 hr posttransfection. Reporter constructs consisted of a basal promoter and the CAT gene either downstream of p53-specific DNA binding sites (p53–CAT), mutant p53 DNA binding sites (mp53–CAT), or the RSV LTR (RSV–CAT). Equal transfection efficiencies of p53–CAT and mp53–CAT transfected cells were determined by CD20 surface staining after cotransfection with a CD20 reporter construct. These data are representative of two independent experiments. (*C*) FL5-Bcl-x_L cells and FL5-Bcl-x_L + DD cells were treated with nocodazole for the indicated times. At each time, cell lysates were made and analyzed by immunoblotting for $p21^{Waf1/Cip1}$.

treatment. Little to no reporter activity was detected in cells transfected with a CAT reporter construct containing mutated p53 DNA binding sites. In addition, $p21^{Waf1/Cip1}$, a direct transcriptional target for p53, was also induced at the protein level by nocodazole treatment (Fig. 3C). Induction of $p21^{Waf1/Cip1}$ after nocodazole treatment is dependent on p53, as no induction was seen in cells transfected with DD.

Abrogation of p53 function and expression of Bcl-x_L cooperatively allow cells with mitotic spindle damage to continue cell cycle progression

The induction of p53 expression after nocodazole treatment suggests that p53 may function in a checkpoint control that prevents cell cycle progression and/or causes apoptosis in cells with a disrupted mitotic spindle. To test this, FL5-Neo + DD and FL5-Neo cells were treated with nocodazole, and cell viabilities and DNA histograms were determined over the course of 72 hr. Expression of DD had only a marginal effect on nocodazole-induced cell death because both FL5-Neo and FL5-

Neo + DD cells died at similar rates over a treatment course of 3 days (Figure 4A).

Despite marginal differences in viability, DD-expressing cells displayed a dramatically different cell cycle profile compared with FL5-Neo cells. In contrast to FL5-Neo cells, which predominantly remained arrested with a 4N DNA content after 72 hr of nocodazole exposure, FL5-Neo + DD cells continued progressing through the cell cycle despite the presence of mitotic spindle damage (Figure 4B). Between 24 and 48 hr, the majority of surviving FL5-Neo + DD cells had a DNA content between 4N and 8N, and at 72 hr, a significant fraction had a >8N DNA content. At the end of 72 hr, 68% of the surviving FL5-Neo + DD cells had a >4N DNA content compared with only 19% of the FL5-Neo cells. These data demonstrate that p53 is a necessary component of a checkpoint control that keeps cells with mitotic spindle damage from reinitiating DNA synthesis.

Because Bcl-x_L expression is able to enhance the accumulation of polyploid cells after mitotic spindle damage despite the induction of functional p53, and because introduction of DD only slightly influences viability after mitotic spindle damage, these results predict that after mitotic spindle damage the loss of p53 and the expression of Bcl-x_L might work in at least an additive fashion to further increase the percentage of cells with a >4N DNA content. To test this, FL5-Bcl-x_L + DD cells were also treated with nocodazole. Figure 4A shows that the viabilities of FL5-Bcl-x_L and FL5-Bcl-x_L + DD cells were similar. Both cell types were >75% viable after 72 hr of nocodazole exposure. However, whereas Bcl-x_L expression alone permitted a gradual increase in 8N cells during the 72-hr time course, Bcl-x_L expression combined with DD allowed rapid accumulation of 8N and then 16N cells. By 72 hr, 86% of FL5-Bcl-x_L + DD cells had a >4N DNA content, and of these cells, most had a >8N DNA content. In contrast, only 52% of FL5-Bcl-x_L cells had a >4N DNA content and few cells had a >8N DNA content. When compared with cells that express DD alone, the introduction of Bcl-x_L into DD-expressing cells enhanced cell viability and the percentage of cells that continued cell cycle progression after mitotic spindle damage (Figures 4A and 4B). The increase in the percentage of cells with a >4N DNA content was not a result of a higher level of DD in FL5-Bcl-x_L + DD cells compared with FL5-Neo + DD cells (Figure 2B). Thus, these data demonstrate that in cells with mitotic spindle damage, the inhibition of p53 function and the prevention of apoptosis through Bcl-x_L expression cooperate to overcome a checkpoint induced by mitotic spindle damage.

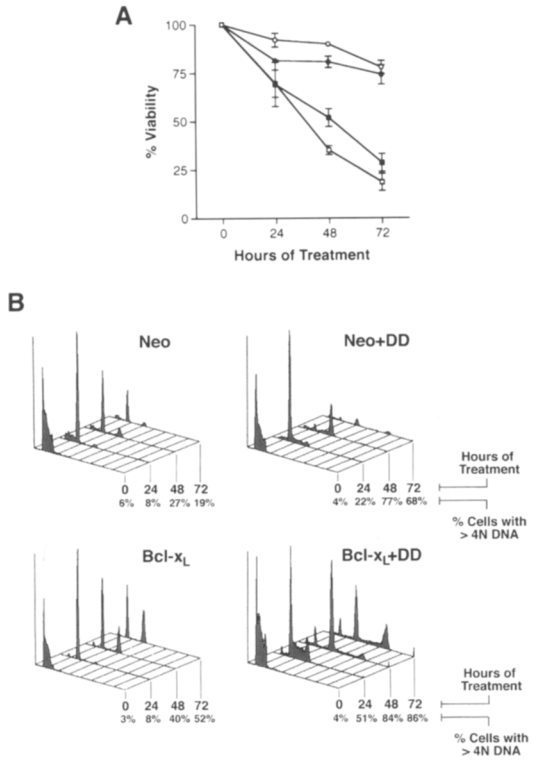

Figure 4. Expression of Bcl-x_L and abrogation of p53 function cooperatively allow accumulation and cell cycle progression of polyploid cells after mitotic spindle damage. (*A*) The indicated cells were treated with nocodazole for 72 hr. Every 24 hr, cell viability was determined by propidium iodide exclusion (means ±S.D., $n = 6$). (○) Bcl-x_L; (●) Bcl-x_L + DD; (□) Neo; (■) Neo + DD. (*B*) The indicated cells were treated with nocodazole for 72 hr. Every 24 hr, cells were harvested and processed for cell cycle analysis by flow cytometry of propidium iodide-stained cells as described in the legend for Fig. 1. These data are representative of at least three independent experiments.

Enforcing p53 levels in Bcl-x_L-expressing cells inhibits cell cycle progression after mitotic spindle damage

It has been demonstrated in many systems that blocking cell death with antiapoptosis genes does not prevent growth arrest (Hockenbery 1995). Therefore, we were interested in understanding why expression of an antiapoptosis gene like *bcl-x_L* resulted in the accumulation of polyploid cells in response to mitotic spindle damage.

The kinetics of p53 expression after nocodazole treatment indicated that p53 levels did not remain elevated during the entire 72 hr of treatment (Figure 3A). The 48 hr time point at which p53 levels began declining coincided with the time at which 4N cells began to accumulate in FL5-Bcl-x_L cultures (Figs. 1 and 4B). This suggests that a potential mechanism by which Bcl-x_L influences the ability of cells to remain arrested is by allowing cells to survive to a point after which p53 is downregulated, perhaps because of adaptation of the checkpoint pathway. Cells that are no longer able to maintain p53 normally would die, but when apoptosis is prevented by Bcl-x_L, these cells proceed to replicate their DNA. As a test of this model, we cotransfected FL5.12 cells with *bcl-x_L* and a temperature-sensitive *p53* (*tsp53*). For this mutant, incubation at the permissive temperature of 32°C leads to high-level expression of p53 in a wild-type conformation, resulting in G_1 arrest (Figure 5, cf. FL5-Bcl-x_L and FL5-Bcl-x_L + tsp53). To determine if maintaining high levels of wild-type p53 in cells expressing Bcl-x_L could inhibit cell cycle progression after mitotic

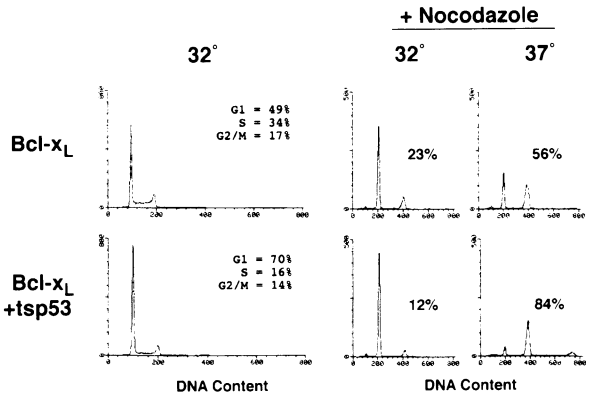

Figure 5. Enforced p53 expression inhibits the ability of Bcl-x_L to promote polyploidy after mitotic spindle damage. FL5.12 cells, stably cotransfected with *bcl-x_L* and a temperature-sensitive *p53* (*bcl-x_L + tsp53*) or transfected with *bcl-x_L* alone (*bcl-x_L*), were either treated with nocodazole for 72 hr or left untreated for 48 hr. One set of duplicate samples were maintained at 37°C and the other set was maintained at 32°C. Cells were then harvested for propidium iodide staining, followed by flow cytometry. The percentage of cells in G_1, S, and G_2/M is indicated in the *upper right* of the DNA histograms from the untreated samples. The percentage of cells with a >4N DNA content are shown for each histogram of the treated samples. These data are representative of three independent experiments performed with two different clones.

spindle damage, FL5-Bcl-x_L + tsp53 cells were treated with nocodazole and shifted to 32°C. As seen in Figure 5, enforced expression of a wild-type form of p53 in FL5-Bcl-x_L + tsp53 cells inhibited cell cycle progression after 72 hr of nocodazole treatment compared with FL5-Bcl-x_L cells. At the restrictive temperature of 37°C, the tsp53 is in a mutant conformation and acts as a dominant negative. Therefore, when compared with cells expressing Bcl-x_L alone, FL5-Bcl-x_L + tsp53 cells at 37°C had an increased percentage of cells with a >4N DNA content after nocodazole treatment, consistent with the data obtained from the DD transfectants. Thus, maintaining high p53 levels at later time points of nocodazole treatment is sufficient to antagonize the ability of Bcl-x_L to promote the accumulation of polyploid cells.

Mitotic spindle damage induces a transient M phase arrest that is not affected by either p53 or Bcl-x_L

The fact that the checkpoint control that is active after mitotic spindle damage is p53 dependent and arrests cells with a 4N DNA content suggests that p53 may be working to arrest cells in mitosis. To determine whether nocodazole-treated cells display a prolonged M-phase arrest, we analyzed three well-characterized M-phase markers: Cyclin B1 expression, MPM-2 expression, and the presence of condensed mitotic chromosomes. FL5-Neo and FL5-Bcl-x_L cells treated with nocodazole demonstrated high levels of Cyclin B1 expression at 8 hr, consistent with an accumulation of cells in M phase (Figure 6A). However, Cyclin B1 levels declined to near interphase levels by 24 hr, demonstrating that the majority of the cells did not remain arrested in mitosis. A Cdc2 immunoblot showed that Cdc2 did not undergo a similar decline in expression, arguing against a general decrease in protein synthesis.

MPM-2 is an epitope whose expression is restricted to M phase (Davis et al. 1983). Flow cytometry on nocodazole-treated cells intracellularly stained for MPM-2 was used to follow the percentage of cells that were in M phase at various times during nocodazole treatment. The left panels of Figure 6B show that at 12 hr, nearly 50% of the FL5-Neo cells were positive for MPM-2, demonstrating that an M-phase arrest did occur; however, the percentage of MPM-2 positive cells began to decline thereafter. By 24 hr of nocodazole treatment, the percentage of cells that were MPM-2 positive was only threefold higher than interphase levels. Thus, the decrease in MPM-2 reactive cells at 24 hr (and at later time points; data not shown), despite evidence of a prolonged p53-dependent cell cycle arrest by DNA staining, suggests

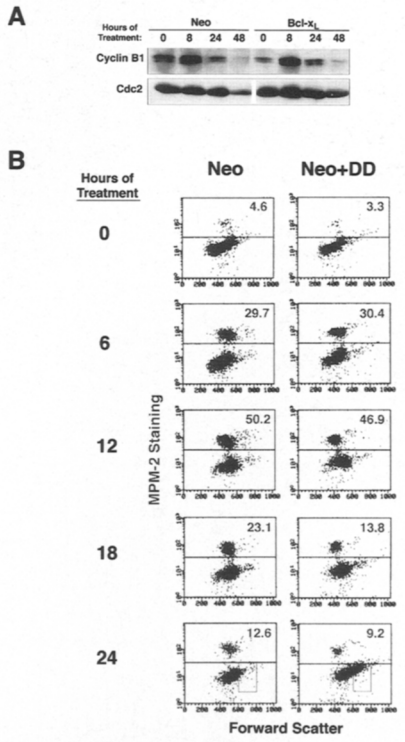

Figure 6. Mitotic spindle damage causes a transient arrest in mitosis as determined by the expression of mitotic proteins. FL5-Neo and FL5-Bcl-x_L cells were treated with nocodazole for the indicated times. (*A*) Cell lysates were made and analyzed by immunoblotting for Cyclin B1 and Cdc2. (*B*) FL5-Neo cells and FL5-Neo + DD cells were analyzed for the percentage of cells in mitosis by flow cytometry of MPM-2 stained cells. Results are plotted with MPM-2 fluorescence on the y-axis and forward scatter on the x-axis. The percentage of cells that are MPM-2 positive is indicated in the *upper right-hand* corner. For the 24 hr time point, a box is drawn that indicates the population of cells that demonstrate an increase in forward scatter. This population comprises 6.4% of the total FL5-Neo population and 22.7% of the total FL5-Neo + DD population. These data are representative of three independent experiments.

that p53 does not cause an extended arrest in mitosis. Consistent with this interpretation, a similar analysis on FL5-Neo + DD cells showed that the kinetics of MPM-2 reactivity was nearly identical to FL5-Neo cells (right panels of Fig. 6B). However, one notable difference is that at 24 hr the FL5-Neo + DD cells contained a large population that was MPM-2 negative and had an increase in cell size as indicated by an increase in forward light scatter (this population is boxed in Fig. 6B). This population likely reflects the failure of FL5-Neo + DD cells to undergo a p53-dependent cell cycle arrest that occurs after a transient M-phase arrest.

To confirm that MPM-2 staining accurately represents mitotic cells, nocodazole-treated cells were stained with both an anti-MPM-2 antibody and DAPI. Confocal microscopy demonstrated that in both FL5-Neo and FL5-Bcl-x_L cells, approximately half of the cells accumulated MPM-2 fluorescence at 16 hr of nocodazole treatment, which is consistent with the flow cytometry analysis (data not shown). These cells all exhibited condensed mitotic chromosomes, and almost all cells that were MPM-2 negative exhibited decondensed chromatin, demonstrating that MPM-2 reactivity and the presence of condensed mitotic chromosomes are nearly always coincidental. In FL5-Neo cells, condensed apoptotic nuclei were also seen. By 24 hr of nocodazole treatment, FL5-Bcl-x_L cells and FL5-Neo cells predominantly exhibited interphase chromatin and were negative for MPM-2.

In response to mitotic spindle damage p53 is not induced in mitosis but during a subsequent growth phase where it mediates cell cycle arrest

Thus far, we have shown that p53 is induced after mitotic spindle damage and its function is important in keeping the damaged cells arrested with a 4N DNA content. However, it would seem that the cells arrested with a 4N DNA content are not necessarily arrested in mitosis. Arrest in mitosis is short and uninfluenced by p53. This suggests that the induction of p53 might occur after cells are released from M-phase arrest. For this reason, nocodazole-treated cells were intracellularly stained with antibodies against both p53 and MPM-2 to test directly whether mitotic cells expressed the induced p53 protein. Figure 7A shows that p53 and MPM-2 staining were mutually exclusive. At 12 hr, MPM-2 staining peaked at 45%, just when p53 staining became detectable. Between 12 and 24 hr, there was a ~37% decrease in MPM-2 positive cells, in contrast to the 27% gain in p53 positive cells. The loss in the percentage of MPM-2 positive cells seen from 12 to 24 hr can be approximately accounted for by the gain in the percentage of p53 positive cells. At no time during the analysis was there a significant percentage of cells expressing both proteins. These data suggest that in response to mitotic spindle damage, p53 is induced after a transient mitotic arrest.

Because the nocodazole-induced M-phase arrest is transient and does not involve p53, we were interested in knowing the cell cycle phase that cells proceed to after M-phase arrest. Based on kinetics, this cell cycle phase is

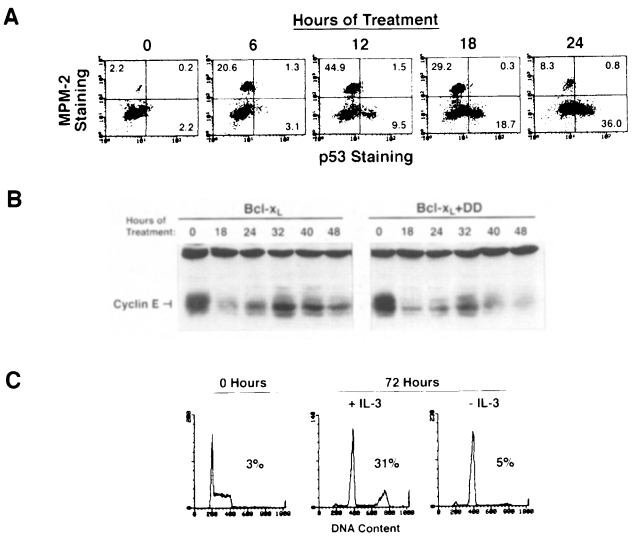

Figure 7. p53 induced after mitotic spindle damage is not expressed in cells arrested in mitosis but instead expressed in a subsequent G_1-like phase. FL5-Bcl-x_L cells were treated with nocodazole for the indicated times. (*A*) These cells were intracellularly stained for both MPM-2 and p53 expression and were analyzed by flow cytometry. MPM-2 fluorescence is on the y-axis and p53 fluorescence is on the x-axis. Quadrants are shown and the percentage of cells in the single-positive populations and the double-positive population is given. (*B*) FL5-Bcl-x_L cells and FL5-Bcl-x_L + DD cells were treated with nocodazole for the indicated times. At each time point, cell lysates were made and analyzed by immunoblotting for Cyclin E. The band at the top of the gel is nonspecific and serves as a loading control. (*C*) At 9 hr after addition of nocodazole, IL-3 was removed from the medium by washing and resuspending the cells in IL-3-free medium containing nocodazole. After 72 hr, cells were harvested and processed for cell cycle analysis by flow cytometry of propidium iodide-stained cells. The percentage of cells with a >4N DNA content is shown. No major differences in cell survival of FL5-Bcl-x_L cells treated in the presence or absence of IL-3 were observed. These data are representative of two independent experiments.

presumably where p53 is induced and mediates cell cycle arrest. The most likely situation is that the transiently arrested cells reset to G_1. To test this, the expression pattern of Cyclin E, a late G_1 cyclin, during nocodazole treatment of FL5-Bcl-x_L cells and FL5-Bcl-x_L + DD cells was analyzed. As seen in Figure 7B, in both FL5-Bcl-x_L cells and FL5-Bcl-x_L + DD cells, nocodazole treatment caused an initial decrease in Cyclin E expression as cells transiently arrested in M phase. However, in both populations of cells, Cyclin E began to reaccumulate after 24 hr of nocodazole treatment. In FL5-Bcl-x_L cells, once Cyclin E reaccumulated its expression was maintained for the rest of the culture period. In contrast, in FL5-Bcl-x_L + DD cells, once reaccumulated, Cyclin E again declined as cells began to resynthesize DNA. These data suggest that cells with mitotic spindle damage undergo a p53-dependent arrest in a state similar to late G_1.

As an independent confirmation that cells with mitotic spindle damage reset to G_1, we took advantage of

the fact that FL5.12 cells are dependent on IL-3 for G_1 cell cycle progression. As seen in Figure 7C, when IL-3 was removed from the media at 9 hr of nocodazole treatment FL5-Bcl-x_L cells did not go on to replicate their DNA. Because IL-3 is necessary for the cells to pass the G_1 restriction point, its requirement for generating cells with a >4N DNA content after mitotic spindle damage further supports that passage through a growth factor-dependent G_1-like phase occurs after the transient mitotic arrest.

Discussion

In this study, we show that mitotic spindle damage activates a checkpoint control that prevents DNA replication of damaged cells by causing p53-dependent cell cycle arrest and p53-independent apoptosis. If cells are prevented from undergoing apoptosis by expression of Bcl-x_L, we find that this promotes the accumulation of polyploid cells. Bcl-x_L does not seem to override the checkpoint induced by mitotic spindle damage but rather allows cells to survive until the p53-dependent arrest pathway either becomes exhausted or undergoes adaptation. Once the p53-dependent checkpoint decays, Bcl-x_L-protected cells replicate their DNA, despite having failed to properly execute the previous M phase. When p53 expression is enforced, resulting in continuously high levels of p53, DNA replication is inhibited. Further evidence that apoptosis is an important mechanism used to prevent polyploidy is the observation that cells that overexpress Bcl-x_L have higher rates of spontaneous tetraploidization.

The finding that p53 is a component of a checkpoint following mitotic spindle damage is consistent with previous reports (Cross et al. 1995). We find that p53 functions to keep cells with spindle damage arrested with a 4N DNA content. The introduction of DD, a dominant negative p53 miniprotein, abrogates the cell cycle arrest observed following mitotic spindle damage. These cells go on to become 8N and then 16N during the 72 hr of nocodazole treatment. During the 72 hr time course, 16N cells are not seen in cells that overexpress Bcl-x_L alone, emphasizing the differences in the way DD and Bcl-x_L function. With Bcl-x_L, cells are rescued from apoptosis and survive long enough to escape cell cycle arrest; however, these cells likely stop at the same checkpoint in the next cell cycle. In contrast, cells with DD lack the p53-mediated arrest altogether and are able to proceed through multiple rounds of DNA replication. However, these cells still lose viability at a rate comparable to wild-type cells.

The inability of DD to prevent apoptosis after mitotic spindle damage suggests that FL5.12 cells undergo cell death via p53-independent mechanisms. DD is able to inactivate p53-mediated apoptosis as demonstrated by experiments analyzing cell death after irradiation and etoposide treatment. Nevertheless, because we have used Bcl-x_L overexpression to prevent apoptosis in our studies and Bcl-x_L overexpression can inhibit both p53-dependent and p53-independent apoptosis, we cannot exclude an additional role for p53-dependent apoptosis in preventing the development of polyploid cells following mitotic spindle damage.

Many reports have suggested that arrest and apoptosis are downstream effects dependent on p53 and important in endowing p53 with tumor-suppressing properties (Cox and Lane 1995; Haffner and Oren 1995). Under circumstances where p53 mediates cell death, cooperation between loss of p53 and overexpression of antiapoptosis genes would not be expected. However, our data suggest that under circumstances where damaged cells undergo p53-independent cell death and p53-dependent cell cycle arrest, the expression of antiapoptosis genes can cooperate with the loss of p53 to enhance the accumulation of genetically damaged cells. Following mitotic spindle damage, p53-dependent growth arrest and p53-independent apoptosis can form a partly redundant checkpoint control system to abort genetically aberrant cells. Cells suffering mitotic spindle damage that are blocked from apoptosis can still cease or dramatically slow proliferation as a result of the arrest pathway. Conversely, cells suffering mitotic spindle damage that are prevented from undergoing growth arrest can still die as a result of the cell death pathway. Elimination of both pathways can cooperatively enhance the ability of cells with mitotic spindle damage to accumulate and progress through the cell cycle.

Recent data have suggested that p53 has a role in G_2 and/or M phase of the cell cycle. p53-null fibroblasts rapidly become polyploid and aneuploid during cell passage (Harvey et al. 1993) or after treatment with a mitotic spindle poison (Cross et al. 1995). Erythroid cell lines from p53 knockout mice are stably diploid but are susceptible to polyploidization (Metz et al. 1995). p53 has been shown to be phosphorylated by G_2/M cyclins, resulting in altered DNA binding specificity (Wang and Prives 1995). p53 expression from an inducible promoter is able to arrest cells in G_2/M (Agarwal et al. 1995). However, despite these observations that seem to support a role for p53 in G_2/M, we fail to observe any evidence for such a role for p53 after mitotic spindle damage.

Our data suggest that in murine cells, M phase-specific checkpoint controls that monitor mitotic spindles, as suggested by studies in yeast (Hoyt et al. 1991; Li and Murray 1991) and *Xenopus* (Minshull et al. 1994) and checkpoints that monitor kinetochores (Li and Nicklas 1995; Rieder et al. 1995) may only lead to a transient mitotic arrest. These data are consistent with previous findings (Kung et al. 1990). However, in addition, we show that this transient M-phase arrest does not involve p53. Rather, after the transient M-phase arrest, cells default to what appears to be a G_1-like phase in which the cells are MPM-2 negative, low in Cyclin B1, high in Cyclin E, and have interphase chromatin. It is at this point that p53 is induced and mediates growth arrest. After mitotic spindle damage, p53 may function in a pathway that senses the consequences of an abortive mitosis. An abortive mitosis may induce p53 due to DNA damage or topological structures caused by the failure to properly segregate sister chromatids. Alternatively, because p53

has been shown to influence centrosome duplication (Fukasawa et al. 1996), the presence of more than one centrosome in a G_1 cell due to mitotic failure may also lead to p53 induction. Thus, true mitotic checkpoints can function to monitor events within M phase to assure proper anaphase, whereas p53 can function subsequently to prevent cells that have failed M phase from reinitiating DNA replication. Figure 8 presents a model that summarizes our findings.

The disruption of genes involved in cell cycle checkpoint controls has long been recognized as one way cells can accumulate karyotypic abnormalities. However, checkpoint controls that simply lead to growth arrest may not be enough to ensure faithful cell division. Our data demonstrate that cell death pathways can also play an important role in preventing the accumulation of genetically abnormal cells. One reason for this may be that in the presence of constant stimuli, checkpoint pathways, like other signal transduction pathways, can undergo adaptation and lose activity (Sandell and Zakian 1993). Apoptosis may provide a mechanism to abort cells before adaptation occurs.

Materials and methods

Cell culture and cell transfections

The murine prolymphocytic IL-3-dependent cell line, FL5.12 was maintained as described previously (Boise et al. 1993). To create FL5-Bcl-x_L or FL5-Neo cell lines, transfection with either pSFFV-Bcl-x_L or pSFFV-Neo (Boise et al. 1993) was performed using 10 μg of plasmid, electroporated into 1×10^7 cells at 960 μF and 250 V. Neomycin-resistant cells were selected with 1 mg/ml G418. Single cell clones from the bulk transfection were derived by limiting dilution cloning. Clones were screened for Bcl-x_L expression by immunoblotting with 2A1, a mouse monoclonal antibody to Bcl-x_L (see below). To create FL5-Neo + DD, FL5-Bcl-x_L + DD, or FL5-Bcl-x_L + tsp53 cell lines, FL5.12 cells were cotransfected with either pCMVDD (Shaulian et al. 1992) or pLTRp53cGval135 (Yin et al. 1992) and either pSFFV-Bcl-x_L or pSFFV-Neo. Clones containing DD were screened by flow cytometry of cells intracellularly stained with PAb421, and clones containing tsp53 were screened by immunoblotting with PAb240. Several clones from all cell lines were used in experiments and were found to give similar results.

For drug treatments, cells were resuspended in medium without G418 at a concentration of 5×10^5 cells/ml, along with nocodazole (Sigma). Various doses of nocodazole were tested from 0.01 to 0.6 μg/ml; however, 0.1 μg/ml was generally chosen for most experiments. Cell death of FL5-Neo and FL5-Neo + DD cells in response to etoposide and irradiation was determined essentially as described previously (Canman et al. 1995). In brief, cells were washed three times and resuspended in medium without IL-3. Cells were then either irradiated with 5 Gy gamma radiation or treated with 1 μg/ml etoposide. Viability was determined at 18 hr as a percentage of an untreated control.

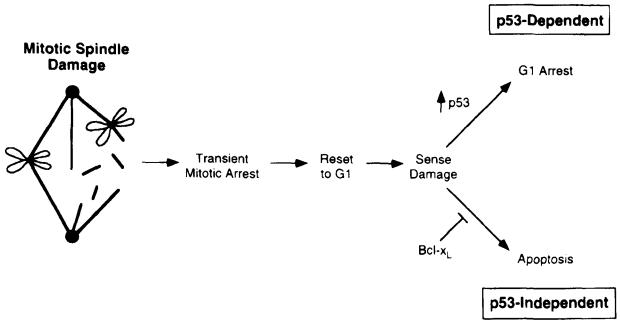

Figure 8. Proposed model for the cellular response to mitotic spindle damage. See text for details.

Cell viability and cell cycle analysis

Cell viability was determined by propidium iodide exclusion, as described previously (Minn et al. 1995). The percent viability was calculated as a percentage of either the viability at 0 hr or the viability of an untreated control. Cell cycle analysis by DNA staining alone was assayed by staining fixed cells with 0.01 mg/ml of propidium iodide. Cells were assayed by flow cytometry and the analysis was gated to exclude subdiploid cells and cell doublets. For cell cycle statistics, data was quantitated with CellFit software (Becton Dickinson) using the RFIT analysis mode. For cell cycle analysis by DNA staining and BrdU incorporation, 1×10^6 cells were pulsed for 30 min with 25 μM of BrdU (Boehringer Mannheim), harvested, and fixed with ethanol. Fixed cells were then washed and incubated in 1 ml of 2.5 M HCl + 0.1% Triton X-100 in PBS for 25 min at room temperature and then washed twice with 4 ml of neutralization/wash solution (0.5% Tween-20 in PBS). The cells were resuspended in 100 μl of antibody staining solution (50% fetal calf serum + 0.01% sodium azide in PBS) along with 4 μl of FITC-conjugated anti-BrdU antibody (Boehringer Mannheim) and incubated at room temperature in the dark for 30 min. Cells were washed twice with PBS and resuspended in 0.5 ml of PBS. Ten micrograms of propidium iodide were added. Samples were then analyzed by flow cytometry.

Immunoblotting

Protein lysates were made by lysing cells in RIPA (150 mM NaCl, 1% NP-40, 0.5% DOC, 0.1% SDS, and 50 mM Tris at pH 7.5) supplemented with 8 μg/ml aprotinin, 2 μg/ml leupeptin, and 170 μg/ml PMSF. Western blots were prepared as described previously (Minn et al. 1995) and blocked with blotto (5% nonfat milk and 0.05–0.2% Tween-20) for 1 hr at room temperature. The blot was then probed with either a 1:10000 dilution of 2A1 (mouse monoclonal anti-Bcl-x_L antibody) (Boise et al. 1995), 1 μg/ml of PAb240 (mouse monoclonal anti-p53 antibody, Santa Cruz), 1 μg/ml of a mouse monoclonal anti-Cyclin B1 antibody (Pharmingen), 1 μg/ml of a mouse monoclonal anti-Cdc2 antibody (#sc-54, Santa Cruz), 0.5 μg/ml of a rabbit polyclonal anti-p21 antibody (#sc-397, Santa Cruz), or 0.5 μg/ml of a rabbit polyclonal anti-Cyclin E antibody (#sc-481, Santa Cruz) for 1 hr at room temperature in blotto. The blot was washed and developed with the ECL system (Amersham).

Intracellular staining for flow cytometry

For intracellular staining, 1×10^6 cells were fixed with 1% paraformaldehyde in PBS for 10 min at room temperature. Cells were then washed in wash solution (0.03% saponin in PBS) and resuspended in 100 μl of staining solution (0.3% saponin and 20% goat serum in PBS) along with 1 μg of PAb421 (Oncogene Science) and/or 0.5 μl of a mouse monoclonal anti-MPM-2 antibody (Upstate Biotechnology) for 30 min at 4°C. Cells were then washed twice with wash solution and resuspended in 100 μl of staining solution without goat serum. For p53 staining or

MPM-2 staining alone, a 1:50 dilution of a FITC-conjugated anti-mouse IgG antibody (Sigma) was used. For p53 and MPM-2 double-staining, a 1:50 dilution of each of a FITC-conjugated anti-mouse IgG2a (Caltag) and a PE-conjugated anti-mouse IgG1 (Caltag) was used. Staining using the secondary antibodies was done for 30 min at 4°C. Cells were then washed twice with wash solution and resuspended in FACS buffer (0.1% sodium azide and 1% BSA in PBS). Cells were then analyzed by flow cytometry.

Chloramphenicol acetyltransferase assay

For CAT assays, cells were grown to 5×10^5 cell/ml and 1×10^7 cells were electroporated with 10 μg of either pPG_{13}-CAT (containing p53 DNA binding sites) or pMG_{15}-CAT (containing mutated p53 DNA binding sites) (Kern et al. 1992) along with 10 μg of pCMVCD20 (Van den Heuvel and Harlow 1993). After 6 hr, 0.1 μg/ml of nocodazole was added to two-thirds of the cells. At 48 hr, cells were stained for CD20 expression using a FITC-conjugated anti-CD20 antibody (Becton Dickinson) and analyzed by flow cytometry for equal transfection efficiencies. Cells were also harvested at 48 hr, washed with PBS, and resuspended in 100 μl of 0.25 M Tris (pH 7.8). Cells were lysed by three rounds of freezeing and thawing, and cellular debris was cleared by centrifugation at 14,000*g* for 5 min at 4°C. Protein concentration was quantitated by Bradford protein assay (Bio-Rad). Seventy micrograms of acetyl CoA and 1 μCi of ^{14}C-chloramphenicol were added to 50 μg of protein in 140 μl of 1M Tris (pH 7.8). The sample was then incubated for 2 hr at 37°C. After ethyl acetate extraction, the organic layer was lyophilized for 15 min, resuspended in 30 μl of ethyl acetate, and spotted on a thin-layer chromatography plate. After separation, the plate was air-dried and exposed to film.

Acknowledgments

The authors would like to thank Drs. Moshe Oren and Ed Harlow for their generous donation of plasmids; Drs. Steve Kron, Nissam Hay, and Tim McKeithan for thoughtful discussions and review of the manuscript; and Therese Conway for editorial assistance. This work was supported in part by research grant PO1 AI35294 from the National Institutes of Health. L.H.B. was supported by a fellowship from the Leukemia Society of America.

The publication costs of this article were defrayed in part by payment of page charges. This article must therefore be hereby marked "advertisement" in accordance with 18 USC section 1734 solely to indicate this fact.

References

Agarwal, M.L., A. Agarwal, W.R. Taylor, and G.R. Stark. 1995. p53 controls both the G2/M and the G1 cell cycle checkpoints and mediates reversible growth arrest in human fibroblasts. *Proc. Natl. Acad. Sci.* **92:** 8493–8497.

Boise, L.H., M. Gonzalez-Garcia, C.E. Postema, L. Ding, T. Lindsten, L.A. Turka, X. Mao, G. Nunez, and C.B. Thompson. 1993. *bcl-x*, a *bcl-2*-related gene that functions as a dominant regulator of apoptotic cell death. *Cell* **74:** 597–608.

Boise, L.H., A.J. Minn, P.J. Noel, C.H. June, M.A. Accavitti, T. Lindsten, and C.B. Thompson. 1995. CD28 costimulation can promote T cell survival by enhancing the expression of Bcl-x_L. *Immunity* **3:** 87–98.

Canman, C.E., T.M. Gilmer, S.B. Coutts, and M.B. Kastan. 1995. Growth factor modulation of p53-mediated growth arrest versus apoptosis. *Genes & Dev.* **9:** 600–611.

Clarke, A.R., C.A. Purdie, D.J. Harrison, R.G. Morris, C.C. Bird, M.L. Hooper, and A.H. Wyllie. 1993. Thymocyte apoptosis induced by p53-dependent and independent pathways. *Nature* **362:** 849–852.

Cox, L.S. and D.P. Lane. 1995. Tumour suppressors, kinases and clamps: How p53 regulates the cell cycle in response to DNA damage. *Bioessays* **17:** 501–508.

Cross, S.M., C.A. Sanchez, C.A. Morgan, M.K. Schimke, S. Ramel, R.L. Idzerda, W.H. Raskind, and B.J. Reid. 1995. A p53-dependent mouse spindle checkpoint. *Science* **267:** 1353–1356.

Davis, F.M., T.Y. Tsao, S.K. Fowler, and P.N. Rao. 1983. Monoclonal antibodies to mitotic cells. *Proc. Natl. Acad. Sci.* **80:** 2926–2930.

Deng, C., P. Zhang, J.W. Harper, S.J. Elledge, and P. Leder. 1995. Mice lacking p21CIP1/WAF1 undergo normal development, but are defective in G1 checkpoint control. *Cell* **82:** 675–684.

Dole, M., G. Nunez, A.K. Merchant, J. Maybaum, C.K. Rode, C.A. Bloch, and V.P. Castle. 1994. Bcl-2 inhibits chemotherapy-induced apoptosis in neuroblastoma. *Cancer Res.* **54:** 3253–3259.

Dole, M.G., R. Jasty, M.J. Cooper, C.B. Thompson, G. Nunez, and V.P. Castle. 1995. Bcl-x_L is expressed in neuroblastoma cells and modulates chemotherapy-induced apoptosis. *Cancer Res.* **55:** 2576–2582.

El-Deiry, W.S., T. Tokino, V.E. Velculescu, D.B. Levy, R. Parsons, J.M. Trent, D. Lin, W.E. Mercer, K.W. Kinzler, and B. Vogelstein. 1993. *WAF1*, a potential mediator of p53 tumor suppression. *Cell* **75:** 817–825.

Evan, G.I., L. Brown, M. Whyte, and E. Harrington. 1995. Apoptosis and the cell cycle. *Curr. Opin. Cell Biol.* **7:** 825–834.

Fisher, D.E. 1994. Apoptosis in cancer therapy: Crossing the threshold. *Cell* **78:** 539–542.

Fukasawa, K., T. Choi, R. Kuriyama, S. Rulong, and G.F. Vande Woude. 1996. Abnormal centrosome amplification in the absence of p53. *Science* **271:** 1744–1747.

Haffner, R. and M. Oren. 1995. Biochemical properties and biological effects of p53. *Curr. Opin. Genet. Dev.* **5:** 84–90.

Harper, J.W., G.R. Adami, N. Wei, K. Keyomarsi, and S.J. Elledge. 1993. The p21 Cdk-interacting protein Cip1 is a potent inhibitor of G1 cyclin-dependent kinases. *Cell* **75:** 805–816.

Hartwell, L.H. and M.B. Kastan. 1994. Cell cycle control and cancer. *Science* **266:** 1821–1828.

Harvey, M., A.T. Sands, R.S. Weiss, M.E. Hegi, R.W. Wiseman, P. Pantazis, B.C. Giovanella, M.A. Tainsky, A. Bradley, and L.A. Donehower. 1993. In vitro growth characteristics of embryo fibroblasts isolated from p53-deficient mice. *Oncogene* **8:** 2457–2467.

Hockenbery, D.M. 1995. *bcl-2*, a novel regulator of cell death. *BioEssays* **17:** 631–638.

Hollstein, M., D. Sidransky, B. Vogelstein, and C.C. Harris. 1991. p53 mutations in human cancers. *Science* **253:** 49–53.

Hoyt, M.A., L. Totis, and B.T. Roberts. 1991. S. cerevisiae genes required for cell cycle arrest in response to loss of microtubule function. *Cell* **66:** 507–517.

Kastan, M.B., Q. Zhan, W.S. El-Deiry, F. Carrier, T. Jacks, W.V. Walsh, B.S. Plunkett, B. Vogelstein, and A.J. Fornace Jr. 1992. A mammalian cell cycle checkpoint pathway utilizing p53 and GADD45 is defective in ataxia-telangiectasia. *Cell* **71:** 587–597.

Kern, S.E., J.A. Pietenpol, S. Thiagalingam, A. Seymour, K.W.

Kinzler, and B. Vogelstein. 1992. Oncogenic forms of p53 inhibit p53-regulated gene expression. *Science* **256:** 827–830.

Kuerbitz, S.J., B.S. Plunkett, W.V. Walsh, and M.B. Kastan. 1992. Wild-type p53 is a cell cycle checkpoint determinant following irradiation. *Proc. Natl. Acad. Sci.* **89:** 7491–7495.

Kung, A.L., S.W. Sherwood, and R.T. Schimke. 1990. Cell line-specific differences in the control of cell cycle progression in the absence of mitosis. *Proc. Natl. Acad. Sci.* **87:** 9553–9557.

Li, R. and A.W. Murray. 1991. Feedback control of mitosis in budding yeast. *Cell* **66:** 519–531.

Li, X. and R.B. Nicklas. 1995. Mitotic forces control a cell-cycle checkpoint. *Nature* **373:** 630–632.

Lowe, S.W., H.E. Ruley, T. Jacks, and D.E. Housman. 1993a. p53-dependent apoptosis modulates the cytotoxicity of anticancer agents. *Cell* **74:** 957–967.

Lowe, S.W., E.M. Schmitt, S.W. Smith, B.A. Osborne, and T. Jacks. 1993b. p53 is required for radiation-induced apoptosis in mouse thymocytes. *Nature* **362:** 847–849.

Lowe, S.W., S. Bodis, A. McClatchey, L. Remington, H.E. Ruley, D.E. Fisher, D.E. Housman, and T. Jacks. 1994. p53 status and the efficacy of cancer therapy in vivo. *Science* **266:** 807–810.

Metz, T., A.W. Harris, and J.M. Adams. 1995. Absence of p53 allows direct immortalization of hematopoietic cells by the myc and raf oncogenes. *Cell* **82:** 29–36.

Minn, A.J., C.M. Rudin, L.H. Boise, and C.B. Thompson. 1995. Expression of Bcl-x_L can confer a multidrug resistance phenotype. *Blood* **86:** 1903–1910.

Minshull, J., H. Sun, N.K. Tonks, and A.W. Murray. 1994. A MAP kinase-dependent spindle assembly checkpoint in Xenopus egg extracts. *Cell* **79:** 475–486.

Miyashita, T. and J.C. Reed. 1993. Bcl-2 oncoprotein blocks chemotherapy-induced apoptosis in a human leukemia cell line. *Blood* **81:** 151–157.

Murray, A.W. 1994. Cell cycle checkpoints. *Curr. Opin. Cell Biol.* **6:** 872–876.

———. 1995. The genetics of cell cycle checkpoints. *Curr. Opin. Genet. Dev.* **5:** 5–11.

Rieder, C.L., R.W. Cole, A. Khodjakov, and G. Sluder. 1995. The checkpoint delaying anaphase in response to chromosome monoorientation is mediated by an inhibitory signal produced by unattached kinetochores. *J. Cell Biol.* **130:** 941–948.

Sandell, L.L. and V.A. Zakian. 1993. Loss of a yeast telomere: Arrest, recovery, and chromosome loss. *Cell* **75:** 729–739.

Schlaifer, D., M. March, S. Krajewski, G. Laurent, J. Pris, G. Delsol, J.C. Reed, and P. Brousset. 1995. High expression of the bcl-x gene in Reed-Sternberg cells of Hodgkin's disease. *Blood* **85:** 2671–2674.

Shaulian, E., A. Zauberman, D. Ginsberg, and M. Oren. 1992. Identification of a minimal transforming domain of p53: Negative dominance through abrogation of sequence-specific DNA binding. *Mol. Cell. Biol.* **12:** 5581–5592.

Smith, M.L., I.T. Chen, Q. Zhan, I. Bae, C.Y. Chen, T.M. Gilmer, M.B. Kastan, P.M. O'Connor, and A.J. Fornace Jr. 1994. Interaction of the p53-regulated protein Gadd45 with proliferating cell nuclear antigen. *Science* **266:** 1376–1380.

Van den Heuvel, S. and E. Harlow. 1993. Distinct roles for cyclin-dependent kinases in cell cycle control. *Science* **262:** 2050–2054.

Wang, Y. and C. Prives. 1995. Increased and altered DNA binding of human p53 by S and G2/M but not G1 cyclin-dependent kinases. *Nature* **376:** 88–91.

Yin, Y., M.A. Tainsky, F.Z. Bischoff, L.C. Strong, and G.M. Wahl. 1992. Wild-type p53 restores cell cycle control and inhibits gene amplification in cells with mutant p53 alleles. *Cell* **70:** 937–948.

Expression of Bcl-xL and loss of p53 can cooperate to overcome a cell cycle checkpoint induced by mitotic spindle damage.

A J Minn, L H Boise and C B Thompson

Genes Dev. 1996, **10:**
Access the most recent version at doi:10.1101/gad.10.20.2621